Fluorine content of SiOF films as determined by IR spectroscopy and resonant nuclear reaction analysis

J. C. Alonso,[a] X. M. Díaz-Bucio, A. Ortiz, and A. Benami
Instituto de Investigaciones en Materiales, Universidad Nacional Autónoma de México, A.P. 70-360, 04510 Mexico Distrito Federal, Mexico

J. C. Cheang-Wong and L. Rodríguez-Fernández
Instituto de Física, Universidad Nacional Autónoma de Mexico, A.P. 20-364, 01000 Mexico Distrito Federal, Mexico

(Received 3 November 2006; accepted 31 January 2007; published 20 March 2007)

In this article, the authors compare the fluorine concentrations obtained from the strength of the infrared-absorption band due to Si–F bonds, with the absolute concentrations determined from $^{19}F(p,\alpha\gamma)^{16}O$ resonant nuclear reaction analysis, for a series of fluorinated silicon oxide (SiOF) films prepared by remote plasma-enhanced chemical-vapor deposition with different flow rates of H_2 in $SiF_4/O_2/He$ mixtures. The authors use this comparison to calibrate the proportionality constant between the strength (integrated absorption) of the infrared-absorption band due to Si–F bonds and the concentration of these bonds in the films. The authors found that (under the Gentzel and Martin approach [Surf. Sci. **34**, 33 (1973)]) this calibration requires the correction of the "fudge" factor, to a new value, $\gamma=1.28$, which is more consistent with the small correction to the local field expected for porous SiOF films. The authors also found that the changes in the refractive index and density of the films introduce less significant corrections in the quantification process of fluorine by the infrared method. © *2007 American Vacuum Society.* [DOI: 10.1116/1.2712195]

I. INTRODUCTION

Fluorinated silicon dioxide (SiOF) and other fluorinated compounds have received much attention as low-dielectric-constant intermetal dielectric layers for reducing the parasitic capacitance of modern high-speed ultralarge-scale integrated circuits.[1–11] SiOF films with low refractive indices are also attractive in optical-layer systems such as antireflective coatings and optical filters.[12] At present, it is well known that the refractive index and dielectric constant of SiOF are proportionally reduced as its F content increases. However, above certain F incorporation, this reduction is accompanied by diverse harmful effects, such as loss of both chemical stability and dielectric integrity.[3–8] Thus, for avoiding and/or controlling these harmful effects, the quantification and control of F content in the SiOF films are very important.

Infrared (IR) spectroscopy is a sensitive, fast, cheap, and nondestructive method which has been widely used for investigating the fluorine dopant level in SiOF films.[1–11,13–16] In most cases, the fluorine content is calculated in terms of the ratio of the area of the IR absorption band related to Si–F bonds to the area of the main IR absorption peak related to Si–O bonds. It is usually underestimated with respect to the fluorine content measured by other techniques, such as Rutherford backscattering.[4] A more careful quantitative analysis of the fluorine content in SiOF films by IR spectroscopy has been made by Han and Aydil,[3] using a relationship between the strength of the infrared-absorption band and density of Si–F bonds, similar to that developed by Brodsky *et al.* for studying the number of silicon-hydrogen bonds in hydrogenated amorphous silicon (a-Si:H) film.[17] However, the calibration and/or adequate correction in the local field approximation, which are/is necessary for an accurate determination of the proportionality constant between integrated absorption and bond concentration,[17,18] have/has not been made for the case of fluorine quantification.

In this work, we compare the fluorine concentrations obtained by Fourier transform infrared (FTIR) absorption spectroscopy for SiOF films deposited by remote plasma-enhanced chemical-vapor deposition (RPECVD) from $SiF_4/H_2/O_2/Ar$ mixtures with those obtained from $^{19}F(p,\alpha\gamma)^{16}O$ resonant nuclear reaction (RNR) analysis. Since the RNR techniques are considered to be some of the most reliable methods for absolute quantitative estimates of fluorine dopant concentration in inorganic materials,[19–21] we use this comparison to calibrate the constants which relate the Si–F IR integrated absorption to fluorine concentration. We also discuss the effect of the changes in the density of the films on the quantification of fluorine and how the calibration of the constants affect the relationship between the applied and local fields under the Gentzel and Martin correction.[17,22]

II. EXPERIMENT

SiOF films with different amounts of incorporated fluorine were deposited in a RPECVD system whose characteristics have been reported elsewhere.[23] He (280 SCCM, where SCCM denotes cubic centimeter at STP) and O_2 (40 SCCM) were fed in the plasma region. SiF_4 (20 SCCM) and H_2 were fed outside the plasma region. Deposits with five different hydrogen flow rates (1, 2, 5, 10, and 20 SCCM) were made in order to change the fluorine content in the

[a]Author to whom correspondence should be addressed; electronic mail: alonso@servidor.unam.mx

 ©2007 American Vacuum Society

TABLE I. Fluorine atom concentrations and atomic percentages, as determined by IR spectroscopy and RNR analysis. IR1 means that the data were calculated using Eqs. (1) and (2) proposed by Han and Aydil (Ref. 3). The refractive index (n') and dielectric constant (ε'_m) of the films obtained from the ellipsometric measurements are also listed.

H_2 flow rate (SCCM)	n'	$\varepsilon'_m = n'^2$	IR1 N_F ($\varepsilon_m = \varepsilon_{SiO_2} = 2.2$) $\times 10^{21}$ (cm^{-3})	IR1 F (at. %) ($\rho_{SiO_2} = 2.2$ g/cm^3)	RNR F (at. %)
1	1.35	1.82	1.43±0.09	6.1±0.4	19.0±2.28
2	1.39	1.93	1.21±0.09	5.4±0.41	16.3±1.96
5	1.41	1.99	0.99±0.07	4.4±0.30	12.0±1.44
10	1.42	2.02	0.75±0.075	3.3±0.33	9.9±1.19
20	1.43	2.04	0.63±0.07	2.8±0.32	5.9±0.71

films. The deposition pressure and plasma power were 500 mTorr and 200 W, respectively. The films were deposited on the polished side of n-type (100) silicon substrates ($\sim 1 \times 1$ cm^2), which were cleaned prior to deposition with semiconductor grade HF diluted in deionized water. The substrate temperature was 200 °C in all cases. The thickness and refractive index of the films were measured by ellipsometry, carried out with a null single-wavelength (632.8 nm) Gaertner L117 ellipsometer. In order to check the reproducibility of the deposition process, three films with different thickness in the range from 100 to 500 nm were deposited for each hydrogen flow rate. The accuracy found in the refractive index was ±0.005 and the error in the thickness was approximately 5%. In order to avoid the loss of fluorine from the SiOF films with a high fluorine content, a very thin film (~30 Å) with the lowest fluorine content (H_2) was deposited on the top surface of the SiOF films. Transmission-infrared-spectroscopy analysis was performed using a FTIR Nicolet 210 spectrophotometer operated in the range of 400–4000 cm^{-1}. Each spectrum was averaged over 200 spectra with a nominal resolution of 4 cm^{-1}. The maximal sensitivity of the FTIR spectrometer was about 0.1% of transmittance. The spectra of the corresponding silicon substrate without film were subtracted from those of the films deposited on the substrates. The area of the 940 cm^{-1} SiF_x absorption band after baseline correction was employed for determining the atomic concentration of $Si-F_x$ units.

The procedure for the absolute measurement of fluorine content in the films was based on the quantification of the 6.92 MeV α particles produced from the $^{19}F(p,\alpha\gamma)^{16}O$ resonant nuclear reaction at a proton (p)-bombarding energy of 1.26 MeV. The RNR analysis experiments were carried out using the 3 MeV Pelletron-tandem accelerator at the Instituto de Física. The α particles emitted in the backward direction (165°) were detected by employing a surface-barrier detector with an area of 150 mm^2, with a 45 μm Mylar filter to stop the backscattered protons. Simultaneous Rutherford backscattering-spectrometry (RBS) measurements from incident protons were made using another detector placed at 168° in order to measure the total atomic-areal density (total number of atoms/cm^2) in the SiOF films. For this analysis, the reference standard was a NdF_3 film deposited by physical-thermal evaporation on a silicon substrate. The fluorine content was additionally measured for some films by quantifying the 6.13 MeV γ rays produced from the same $^{19}F(p,\alpha\gamma)^{16}O$ resonant nuclear reaction. Since this reaction has a very sharp resonance around a p-bombarding energy of 340.5 keV, this reaction has the advantage that the fluorine content can be calculated at different depths and/or along all the thickness of the film, giving rise to depth profiles. These experiments were made in the 700 kV Van de Graaff accelerator (also located at the Instituto de Física). In this case, the γ rays emitted in the forward direction (0° laboratory angle) were detected with a 5.1-cm-diameter by 5.1-cm-thick NaI(Ti) scintillation detector placed as close as possible to the sample. The γ ray yield Y_F (defined as $Y_F \equiv$ number of γ ray counts/number of incident protons) from each film as a function of proton energy (excitation curve) was obtained automatically using a computer program. For each measured point of the excitation curve, a short pulse of protons (1×10^{-6} s) with a dose of 5 μC was used. Absolute quantification of the atomic fraction of F in the SiOF films was made by comparison of Y_F with the gamma yield from a reference standard Y_S having a known fraction f of fluorine. For this analysis, the reference standard was AlF_3.

III. RESULTS

A. Refractive index and dielectric constant

Table I shows the average refractive index, n', and the electronic dielectric constant, $\varepsilon'_m = (n')^2$, of the SiOF films deposited under the different H_2 flow rates. As can be seen, the refractive index and dielectric constant increase as the hydrogen flow rate increases. This result is quite expected, since it is well known that hydrogen scavenges fluorine atoms from the growing SiOF film during deposition through the formation of volatile HF. Thus, as the hydrogen flow rate increases, the amount of fluorine incorporated in the films is reduced and their refractive index increases toward the value corresponding to SiO_2 ($n = 1.46$).

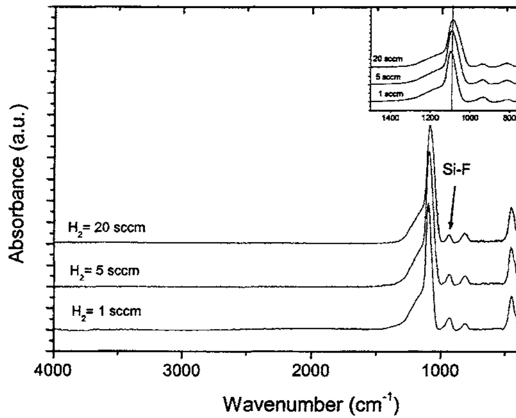

FIG. 1. Absorbance IR spectra of SiOF deposited under different hydrogen flow rates. The intensity of the absorption band associated with SiOF bonds, located around 935 cm^{-1}, increases as the hydrogen flow rate decreases. The inset shows a magnified view of the region between 1500 and 750 cm^{-1} and illustrates that the frequencies of Si–O–Si bond stretching vibrations also increases as the hydrogen flow rate decreases.

B. Quantification of fluorine by FTIR analysis

Figure 1 shows typical FTIR absorbance spectra for SiOF films approximately 450 nm in thickness deposited with three different H_2 flow rates. The inset of this figure shows a magnified view of the region between 1500 and 750 cm^{-1}. The complete spectra show three absorption bands located approximately at 1090, 810, and 454 cm^{-1}, which are characteristic of stretching, bending, and rocking of Si–O bond vibrations, respectively.[24,25] Another band located at approximately 935 cm^{-1} is associated with Si–F bond vibrations. It is observed that the intensity of the Si–F absorption peak decreases as the hydrogen flow rate increases. Consistent with the reduction in the amount of Si–F bonds incorporated in the films, the peak of the Si–O bond stretching vibrations is shifted toward lower frequencies as the hydrogen flow rate increases.[14,15]

The concentration of Si–F bonds in the films as a function of hydrogen flow rate was calculated from the corresponding IR absorbance spectrum by applying the formula previously used by Han and Aydil for calculating the number of Si–F bonds per unit volume in a SiO_2 matrix:[3]

$$N_{\mathrm{F}}(\mathrm{cm}^{-3}) = \gamma \frac{(1+2\varepsilon_m)^2\sqrt{\varepsilon_m}N_A}{9\varepsilon_m^2(\Gamma/\zeta)}\int_{\tilde{\nu}_1}^{\tilde{\nu}_2}\frac{\alpha(\tilde{\nu})}{\tilde{\nu}}d\tilde{\nu} \tag{1}$$

in which the absorptivity $\alpha(\tilde{\nu})$ is divided by the wave number $\tilde{\nu}$ and integrated over the Si–F absorption band located between $\tilde{\nu}_1 < 935\ \mathrm{cm}^{-1} < \tilde{\nu}_2$; and Γ, ζ, N_A, and ε_m, are the absorption cross section for SiF_4 in units of $cm^2/mmol$, the number of Si–F bonds per SiF_4 molecule, Avogadro's number per millimol (mmol), and the electronic-dielectric constant of the SiO_2 matrix, respectively. γ is a "fudge" factor that takes into account inadequacies in the local field correction.[3,17,18] Given that the absorptivity coefficient $\alpha(\tilde{\nu})$ is related to the measured IR absorbance $A(\tilde{\nu})$ by the formula $\alpha(\tilde{\nu})=A(\tilde{\nu})/d$, where d is the film thickness in centimeter, and according to the values used by Han and Aydil:[3] $\Gamma=58.4\ \mathrm{cm}^2/\mathrm{mmol}$, $\zeta=4$, $\varepsilon_m=2.2$, $\gamma=0.5$, and $N_A=6.022\times 10^{20}$ atoms/mmol, Eq. (1) can be expressed as

$$N_{\mathrm{F}}(\mathrm{cm}^{-3}) = 2.0\times 10^{19}(\mathrm{cm}^{-2})\frac{1}{d\tilde{\nu}_{\mathrm{peak}}}\int A(\tilde{\nu})d\tilde{\nu}. \tag{2}$$

This equation allows us to quantify the concentration of Si–F bonds, N_{F}, in terms of the measurable quantities $\tilde{\nu}_{\mathrm{peak}} \sim 935\ \mathrm{cm}^{-1}$, $A(\tilde{\nu})$, and d.

Then the atomic percentage of SiF_x bonds, F (at. %), in the films was calculated using the equation[3]

$$\mathrm{F(at\ \%)} = \frac{N_{\mathrm{F}}}{N_{\mathrm{F}}+N_{\mathrm{SiO_2}}}\times 100\,\%\,, \tag{3}$$

where $N_{\mathrm{SiO_2}}$ is the concentration of Si and O atoms in the SiO_2 matrix. Assuming, as Han and Aydil did, that $\rho_{\mathrm{SiO_2}}=2.2\ \mathrm{g/cm^3}$ and $\mu_{\mathrm{SiO_2}}=60.08$ uma $(1\ \mathrm{uma}=1.66\times 10^{-24}\ \mathrm{g})$, this concentration takes the value $N_{\mathrm{SiO_2}}=\rho_{\mathrm{SiO_2}}/\mu_{\mathrm{SiO_2}}=2.2\times 10^{22}\ \mathrm{cm}^{-3}$.

Table I shows the average concentrations (N_{F}) of SiF bonds and atomic percentages of fluorine (F at. %) in the SiOF films as a function of the hydrogen flow rate used during deposition, calculated using Eq. (2) and (3), respectively. As this table shows, the F at. % decreases from 6.1 to 2.8 at. % as the hydrogen flow rate increases from 1 to 20 SCCM.

C. Quantification of fluorine by RNR analysis

The absolute fluorine content in atoms/cm^2 in the SiOF films was determined from the 6.92 MeV α particles generated by the $^{19}\mathrm{F}(p,\alpha\gamma)^{16}\mathrm{O}$ ($E_p=1.26$ MeV) resonant nuclear reactions using the formula

$$N_{\mathrm{F}}^{\mathrm{SiOF}} = \frac{Y_{\alpha}^{\mathrm{SiOF}}Q^{\mathrm{std}}}{Y_{\alpha}^{\mathrm{std}}Q^{\mathrm{SiOF}}}N_{\mathrm{F}}^{\mathrm{std}}, \tag{4}$$

where $N_{\mathrm{F}}^{\mathrm{SiOF}}$ and $N_{\mathrm{F}}^{\mathrm{std}}$ are the areal densities (number of atoms/cm^2) of fluorine in the SiOF film and standard, respectively, and $Y_{\alpha}^{\mathrm{SiOF}}$ and $Y_{\alpha}^{\mathrm{std}}$ are the yields (number of α particles on counts) for the SiOF film and standard, respectively. Q^{SiOF} and Q^{std} are the accumulated charges (number of protons impinged) on the SiOF film and the standard, respectively.

The fluorine content in atomic percentage ($\%\mathrm{F}_{\alpha}$) is then given by the equation

$$\%\mathrm{F}_{\alpha} = \frac{N_{\mathrm{F}}^{\mathrm{SiOF}}}{N_{T}^{\mathrm{SiOF}}}\times 100, \tag{5}$$

where N_{T}^{SiOF} is the total atomic-areal density of atoms in the SiOF films, which was measured simultaneously by RBS of protons. These fluorine atomic percentages, as a function of hydrogen flow rate, are listed in Table I. In this case, as the hydrogen flow rate increased from 1 to 20 SCCM, the F at. % decreased from 19.0 to 5.9 at. %.

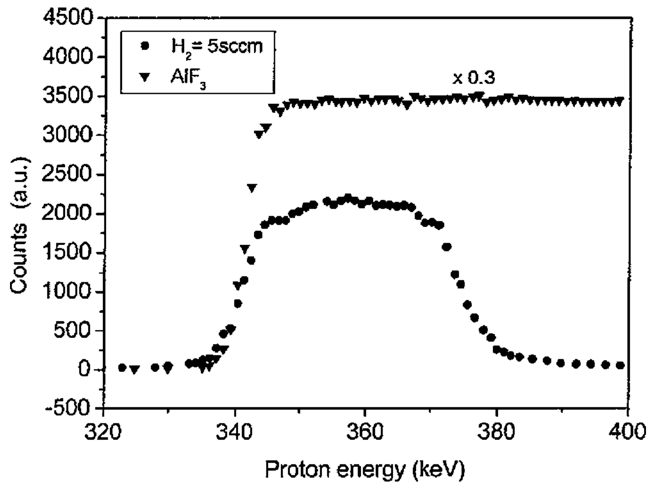

FIG. 2. γ ray depth profile generated by the $^{19}F(p,\alpha\gamma)^{16}O$ (E_p=340.5 keV) resonant nuclear reactions from a SiOF film deposited with the intermediate hydrogen flow rate of 5 sccm. The depth profile of the γ yield (multiplied by 0.3) generated from the AlF_3 standard is also shown.

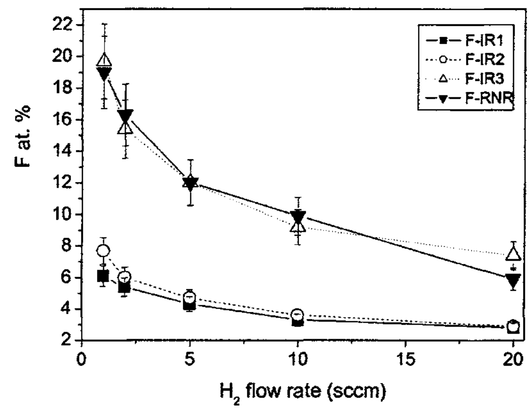

FIG. 3. F at. % as a function of hydrogen flow rate as determined by IR absorption strength method, using (a) the Han and Aydil (Ref. 3) parameters without any correction (data F-IR1, ■ symbol), (b) corrections due to changes in the density of the films according to the Gladstone-Dale approach (data F-IR2, ○ symbol), (c) corrections to the local electric field, through the "fudge" factor (γ=1.28) (data F-IR3, △ symbol), and (d) F at. % absolute values obtained using $^{19}F(p,\alpha\gamma)^{16}O$ resonant nuclear reactions (data F-RNR, ▼ symbol).

The fluorine content ($\%F_\gamma$) in the films was also measured using the 6.13 MeV γ ray depth profiles generated by the $^{19}F(p,\alpha\gamma)^{16}O$ (E_p=340.5 keV) resonant nuclear reactions. In this case, we used the formula

$$\%F_\gamma = \frac{Y_\gamma^{\mathrm{SiOF}} f_{\mathrm{std}} \varepsilon_{\mathrm{SiO_2}}}{Y_\gamma^{\mathrm{std}} \varepsilon_{\mathrm{std}} + f_{\mathrm{std}} Y_\gamma^{\mathrm{SiOF}} (\varepsilon_{\mathrm{O}} - \varepsilon_{\mathrm{F}})} \times 100, \quad (6)$$

where Y_γ^{SiOF} and Y_γ^{std} are the yields (number of γ rays on counts) for the SiOF film and standard, respectively; $\varepsilon_{\mathrm{SiO_2}}$, $\varepsilon_{\mathrm{std}}$, ε_{O}, and ε_{F} are the stopping power of SiO_2, standard, oxygen, and fluorine, respectively; and f_{std} is the fluorine fraction in the standard. In this case, the advantage is that the fluorine content can be calculated at different depths and/or along all the thickness of the film.

Figure 2 shows the γ ray depth profile obtained for a SiOF film deposited with the intermediate hydrogen flow rate of 5 SCCM. The depth profile of the γ yield (multiplied by 0.3) generated from the AlF_3 standard is also shown in Fig. 2. As can be seen, the fluorine content close to the outer surface of the film is lower than that in the bulk. This is due to the protective thin film (with lower fluorine content) deposited on its top surface. At the SiOF/Si substrate interface, there is also a thin zone with a lower fluorine content which is very probably due to diffusion of fluorine toward the native silicon-dioxide thin film. The fluorine content in this film, determined from the whole depth profile shown in Fig. 2, was 12.07 at. %, which is in very good agreement (considering the uncertainty) with the value obtained with alpha particles.

IV. DISCUSSION

The data appearing in Table I, of F at. % as a function of hydrogen flow rate obtained by the previous IR and RNR methods, are plotted in Fig. 3, and they are denoted as F-IR1 (■ symbol) and F-RNR (▼ symbol), respectively. As Table I and Fig. 3 show, the fluorine atomic percentages measured by IR and RNR follow approximately the same trend as a function of hydrogen flow rate. However, the F at. % values measured by IR analysis (2.8–6.1 at. %) are lower than those measured by RNR (5.9–19.0 at. %). As mentioned in the Introduction, a similar underestimation of fluorine content by IR spectroscopy (1–5 at. %) with respect to that determined by Rutherford backscattering (3.5–14 at. %) has been reported in a previous work.[4] It must be pointed out that, given the flow rates of SiF_4 (20 SCCM) and O_2 (40 SCCM) used for the deposition of our SiOF films and that since hydrogen removes fluorine from the films by the formation of HF, a very high incorporation of fluorine atoms is expected in those films deposited with the lowest hydrogen flow rate (1 SCCM). A simple chemical balance of the reactants and products shows that the incorporation of one fluorine atom per silicon atom is highly probable. In theory, according to the pseudobinary alloy representation, when one F atom per Si atom is incorporated in the entire SiO_2 network, the composition of the alloy would be $SiO_{3/2}F$, which corresponds to a fluorine content of 28.6 at. %.[11,14,15] Thus, the value of 19 at. % obtained from RNR analysis for the film deposited under the lowest hydrogen flow rate is much more acceptable than that of 6.1 at. % obtained by IR analysis. Based on this, and since the RNR methods applied in this work are nondestructive and make use of standards, the F at. % values obtained from these methods were used as absolute values to calibrate the IR method.

As Eqs. (2) and (3) show, the F at. % calculated by the IR method can be increased by increasing the proportionality constant in Eq. (2) and/or by decreasing the term $N_{\mathrm{SiO_2}}$ in Eq. (3). Since it is well known that the incorporation of fluorine produces porosity in the SiOF films and/or reduction of their density, before calibrating the proportionality constant in Eq. (2), we proceed to make the corrections due to the changes in density of Si and O atoms.

TABLE II. Flourine atomic percentages as determined by IR spectroscopy, including corrections due to changes in the density of the films (IR1) and after correcting the "fudge" factor (IR2).

H_2 flow rate (SCCM)	Refractive index, n'	Pore fraction, f_m	ρ_{GD} (g/cm^3)	ρ_{lm} (g/cm^3)	IR2 F_{GD} (at. %) $\gamma=0.5$	IR3 F_{GD} (at. %) $\gamma=1.28$
1	1.35	0.18	1.7	1.8	7.7±0.5	19.7±1.28
2	1.39	0.11	1.9	2.0	6.0±0.45	15.4±1.6
5	1.41	0.066	2.0	2.1	4.7±0.32	12.0±0.82
10	1.42	0.052	2.0	2.1	3.6±0.36	9.2±0.92
20	1.43	0.046	2.1	2.1	2.9±0.33	7.4±0.84

A. Corrections due to changes in the density of the films

In order to make this correction, the mass density of the films was estimated using two different approaches. One was based on the empirical equation of Gladstone-Dale, $\rho_{GD}=-4.784+4.785n'$,[26,27] where the values of n' for the SiOF are those listed in Table I. The other approach was based on the linear law of two-phase mixing, $\rho_{lm}=f_p\rho_p+(1-f_p)\rho_{SiO_2}$,[28] where f_p and ρ_p are the volume proportion and density of pores, respectively, and $\rho_{SiO_2}=2.2$ g/cm^3 is the density of SiO_2. For this approach, we used the volume proportion of pores as a function of refractive index (predicted in a previous work[11]) and $\rho_p=\rho_{air}=0.001$ g/cm^3. The concentration of Si and O atoms in the SiOF films was then calculated using the formula $N_{SiO_2}=\rho_{SiOF}/60.08$ uma in Eq. (3).

The mass densities of the films calculated from these approaches are shown in Table II. As can be seen, the Gladstone-Dale densities are slightly lower than those calculated from the linear law approach, and therefore, the former produce a more significant increase in the F at. % values. However, as Table II and Fig. 3 show, the Gladstone-Dale-IR corrected F at. % values [denoted as F-IR2 (○ symbol) in Fig. 3] are still lower than the RNR values.

B. Corrections due to changes in the refractive index of the films

According to Eq. (1), one possible source of error in the quantification of fluorine content by IR analysis is the variation of the refractive index of the films with the fluorine content. However, the use of the values listed in Table I for the refractive index n' and electronic dielectric constant $\varepsilon'_m=(n')^2$ of the films in Eq. (1), instead of the constant values for SiO_2 ($\varepsilon_m=\varepsilon_{SiO_2}=2.22$), did not significantly change the multiplicative factor (2.0×10^{19} cm^{-2}) of Eq. (2), and consequently, the corresponding calculated concentrations (N'_F) and atomic percentages (F′) of fluorine were practically the same.

C. Corrections due to the Γ/ζ parameter

The other physical parameters that allow further correction are the Γ, ζ, and γ parameters appearing in Eq. (1). With respect to the Γ/ζ parameter, there is a little margin of correction, since this is an empirical parameter measured for gaseous SiF_4.[29–31] The fact that the empirically measured value ($\Gamma/\zeta=3.5$ cm^2/mmol) for several silane gases (Si_xH_y) remains constant, independent of x and y, and depends only on the type of bond (Si–H in that case) gives some support to assume that in the case of SiF_4, the value $\Gamma/\zeta=14.6$ cm^2/mmol used in Eq. (1) to obtain Eq. (2) is correct.

D. Corrections due to the local field approach

The remaining parameter to be corrected in Eq. (1) is the γ parameter or fudge factor. With respect to this, it is important to mention that Eq. (1) comes from the general relationship proposed by Brodsky *et al.* for calculating the number of Si–H bonds in amorphous silicon:[17]

$$N(\mathrm{cm}^{-3}) = \frac{\sqrt{\varepsilon_m}N_A}{(e_s^*/e_G^*)^2(\Gamma/\zeta)}\int_{\tilde{\nu}_1}^{\tilde{\nu}_2}\frac{\alpha(\tilde{\nu})}{\tilde{\nu}}d\tilde{\nu} = B\frac{\sqrt{\varepsilon_m}N_A}{(\Gamma/\zeta)}\int_{\tilde{\nu}_1}^{\tilde{\nu}_2}\frac{\alpha(\tilde{\nu})}{\tilde{\nu}}d\tilde{\nu}, \quad (7)$$

where e_S^* is the appropriate effective charge for the relevant bond (Si–H in the case of Brodsky, or Si–F in our case) in a solid matrix of dielectric constant ε_m, and e_G^* is the effective charge for the same bond in vacuum or a dilute gas with refractive index $n=1$. These effective charges are different because in the solid, the local field ($\mathbf{E_s}$) differs from the macroscopic applied field in vacuum ($\mathbf{E_o}$), and for finding the relationship between them, a local field correction or approximation must be made.[17]

The local field correction used by Brodsky for deducing Eq. (7) was originally given by Genzel and Martin. It assumes that the local field $\mathbf{E_s}$ is the same local electric field ($\mathbf{E_i}$) inside a spherical void embedded in a medium of dielectric constant ε_m. In this case the local electric field ($\mathbf{E_s}=\mathbf{E_i}$) (and therefore the effective charge) in the solid is enhanced with respect to the macroscopic field in vacuum ($\mathbf{E_o}$) by the enhancement factor[17,22,32]

$$C_{GM} = \frac{e_S^*}{e_G^*} = \frac{\mathbf{E}_i}{E_o} = \frac{3\varepsilon_m}{(1+2\varepsilon_m)}. \quad (8)$$

This enhancement factor gives rise to the constant

$$B_{\rm GM}=\frac{1}{(C_{\rm GM})^2}=\left(\frac{e_G^*}{e_S^*}\right)^2=\frac{(1+2\varepsilon_m)^2}{9\varepsilon_m^2},\tag{9}$$

which, when substituted in Eq. (7), gives rise to Eq. (1), but without the γ parameter. However, after the original work, it was recognized that this method of determining the hydrogen content in a-Si:H fims was fraught with uncertainty. This was because for high hydrogen contents, a more accurate approximation was proposed by Connell and Pawlik (CP) (Szigeti-type correction),[17,33] in which the solid is supposed to be composed of isotropically distributed polarizable dipoles and the enhancement factor is given by

$$C_{\rm CP}=\frac{e_S^*}{e_G^*}=\frac{\mathbf{E}_i}{E_o}=\frac{\varepsilon_m+2}{3}.\tag{10}$$

In this case, the constant appearing in Eq. (1) would be

$$B_{\rm CP}=\left(\frac{e_G^*}{e_S^*}\right)^2=\frac{9}{(\varepsilon_m+2)^2}.\tag{11}$$

It can be seen from Eq. (9) and (11) that, for a-Si:H (ε_m=12), the enhancement factor of Genzel and Martin ($C_{\rm GM}$=1.44) is lower than that of Connel and Pawlik ($C_{\rm CP}$=4.67), and consequently, the difference between both types of corrections reaches an order of magnitude ($B_{\rm CP}$ =0.046 and $B_{\rm GM}$=0.48) for the calculation of hydrogen concentration.

In a later work, Fang *et al.*[18] applied Eq. (7) under the Genzel and Martin local-field approach to calculate the hydrogen concentration for a-Ge:H (ε_m=16) and a-Si:H (ε_m=12) films from the strength of the infrared stretching and wagging absorption bands and compared these results with absolute measurements of hydrogen content obtained by RNR techniques. This comparison gave rise to the necessity of introducing the γ parameter in Eq. (1), with a value γ=0.5.[18] It must be pointed out that the introduction of this fudge factor was made as an additional correction to the local field, such that the corrected enhancement factor is now

$$C'_{\rm GM}=\frac{e_S^{*\prime}}{e_G^*}=\frac{\mathbf{E}'_i}{E_o}=\frac{1}{\sqrt{\gamma}}\frac{3\varepsilon_m}{(1+2\varepsilon_m)}.\tag{12}$$

In other words, the factor $1/\sqrt{\gamma}$ was a way of taking into account the inadequacies of the Genzel and Martin model to calculate the local field inside the solid a-Si:H and/or a-Ge:H films.

In the case of a-Si:H, the Genzel and Martin model with the addition of the fudge factor with the value γ=0.5 is physically reasonable because it produces the value $C'_{\rm GM}$ =2.04 for the local field-enhancement factor, which is in between $C_{\rm GM}$=1.44 and $C_{\rm CP}$=4.67.

The IR strength [Eq. (1)] and the same fudge factor, γ=0.5, were then used in other works, without any additional justification, for measuring the fluorine content in amorphous fluorinated silicon, a-Si:F(ε_m=12), and SiOF films.[3,29,30] However, we believe that it is not correct to use this value for SiOF films because they have different dielectric properties and structure than a-Si:H and a-Si:F films. Due to the low electronic-dielectric constant ($\varepsilon_m \leq 2$) and the porosity in the SiOF films generated by the fluorine incorporation, it is expected that they be much less polarizable. Consequently, the local internal field should be very close to the external field. In other words, the local field-enhancement factor for these films should be close to unity.

Our results show that the value of γ=0.5 in Eq. (1) gives rise to underestimated fluorine contents (see Table II). Also, in this case, the corresponding corrected enhancement factor given by the Gentzel and Martin approach [Eq. (12)] takes the value of $C'_{\rm GM}\approx 1.7$ for $\varepsilon_m \approx 2$. We believe that due to the porosity of the SiOF films, the use of the Gentzel and Martin approach is a good one because it assumes that the Si–F bonds are inside spherical voids embedded in a medium of dielectric constant ε_m. However, the value of the fudge factor γ=0.5 is unacceptable because it produces an inconsistent increase of the local field-enhancement factor.

On the other hand, as Table II shows, the value of γ required for calibrating the IR fluorine content of the film deposited with the intermediate flow rate (5 SCCM), with the corresponding absolute value obtained by RNR analysis, was γ=1.28. In this case, the corrected enhancement factor given by the Gentzel and Martin approach [Eq. (12)] takes the value of $C'_{\rm GM}\approx 1.06$ for $\varepsilon_m \approx 2$, which is closer to unity.

Therefore, we can conclude that the calibrated value, γ=1.28, is a more acceptable value for the fudge factor for quantifying the fluorine content in SiOF films by IR spectroscopy. In this case, the relationship between the strength of the infrared absorption band and density of Si–F bonds is

$$N_{\rm F}({\rm cm}^{-3})=5.12\times 10^{19}({\rm cm}^{-2})\frac{1}{d\tilde{\nu}_{\rm peak}}\int_{\tilde{\nu}_1}^{\tilde{\nu}_2}A(\tilde{\nu})d\tilde{\nu}.\tag{13}$$

As Fig. 3 shows, the data (F-IR3, Δ symbol) of the F at. % values obtained from Eq. (13) instead of Eq. (2), and using Eq. (3) with the Gladstone-Dale corrections to the atomic density, are in very good agreement with the absolute values obtained by RNR for films with high fluorine content. We hope that this calibration will help to make fast and more reliable measurements by IR absorption spectroscopy of the real limits of fluorine content in SiOF films, where their properties start deteriorating.

V. CONCLUSION

We have compared the fluorine concentrations obtained from the strength of the infrared-absorption band due to Si–F bonds with the absolute concentrations determined from $^{19}{\rm F}(p,\alpha\gamma)^{16}{\rm O}$ resonant nuclear reactions (RNR) analysis for a series of fluorinated silicon-oxide (SiOF) films with different fluorine content. From this comparison we have found that the use of the Gentzel and Martin approach and γ=0.5 for the fudge factor gives rise to underestimated values of fluorine content in SiOF films, as determined from the integrated Si–F IR absorption band. We show that the calibrated value γ=1.28, which reproduces more closely the absolute fluorine contents in these films, is consistent with the small corrections expected for the local field inside these porous, low-dielectric-constant SiOF films. Although corrections due

to the changes in the refractive index and density of the SiOF films must also be taken into account for the quantification of fluorine content by the IR method, these corrections are less significant.

ACKNOWLEDGMENTS

The authors acknowledge the technical assistance of M. A. Canseco, J. Camacho, S. Jimenez, J. C. Pineda, K. López, and F. J. Jaimes, and the partial financial support for this work from CONACyT-México under Project No. 47303-F.

[1]R. K. Laxman, A. K. Hochberg, D. A. Roberts, R. N. Vrtis, and S. Ovalle, Adv. Mater. Opt. Electron. **6**, 93 (1996).
[2]S. W. Lim, Y. Shimogaki, Y. Nakano, K. Tada, and H. Komiyama, Jpn. J. Appl. Phys., Part 1 **35**, 1468 (1996).
[3]S. M. Han and E. S. Aydil, J. Vac. Sci. Technol. A **15**, 2893 (1997).
[4]M. K. Bhan, J. Huang, and D. Cheung, Thin Solid Films **308/309**, 507 (1997).
[5]H. Yang and G. Lucovsky, J. Vac. Sci. Technol. A **16**, 1525 (1997).
[6]V. Pankov, J. C. Alonso, and A. Ortiz, J. Appl. Phys. **86**, 275 (1999).
[7]V. Pankov, J. C. Alonso, and A. Ortiz, J. Vac. Sci. Technol. A **17**, 3166 (1999).
[8]M. T. Mocella, J. Fluorine Chem. **122**, 87 (2003).
[9]G. Power, J. K. Vij, and M. Shaw, J. Phys. D **37**, 1362 (2004).
[10]Y. L. Cheng, Y. L. Wang, H. W. Chen, J. L. Lan, C. P. Liu, S. A. Wu, Y. L. Lo, and M. S. Feng, J. Vac. Sci. Technol. A **22**, 494 (2004).
[11]J. C. Alonso, X. M. Diaz-Bucio, E. Pichardo, L. Rodríguez-Fernández, and A. Ortiz, Thin Solid Films **474**, 294 (2005).
[12]J. K. Kim, S. H. Jeong, B. S. Kim, and S. H. Shim, J. Phys. D **37**, 2425 (2004).
[13]R. Swope and W. S. Yoo, J. Vac. Sci. Technol. B **14**, 1702 (1996).
[14]G. Lucovsky and H. Yang, J. Vac. Sci. Technol. A **15**, 836 (1997).
[15]G. Lucovsky and H. Yang, Jpn. J. Appl. Phys., Part 1 **36**, 1368 (1997).
[16]B. G. Kim, S. Y. Kang, and J. J. Kim, J. Phys. D **30**, 1720 (1997).
[17]M. H. Brodsky, M. Cardona, and J. J. Cuomo, Phys. Rev. B **16**, 3556 (1977).
[18]C. J. Fang, K. J. Gruntz, L. Ley, M. Cardona, F. J. Demon, G. Muller, and S. Kalbitzer, J. Non-Cryst. Solids **35–36**, 255 (1980).
[19]D. Dieumegard, Nucl. Instrum. Methods **168**, 93 (1980).
[20]S. Croft, Nucl. Instrum. Methods Phys. Res. A **307**, 353 (1991).
[21]G. E. Coote, Nucl. Instrum. Methods Phys. Res. B **66**, 191 (1992).
[22]L. Gentzel and T. P. Martin, Surf. Sci. **34**, 33 (1973).
[23]V. Pankov, J. C. Alonso, and A. Ortiz, Jpn. J. Appl. Phys., Part 1 **37**, 6135 (1998).
[24]A. C. Adams, Solid State Technol. **26**, 135 (1983).
[25]P. G. Pai, S. S. Chao, Y. Takagi, and G. Lucovsky, J. Vac. Sci. Technol. A **4**, 689 (1986).
[26]W. A. Pliskin, J. Vac. Sci. Technol. **14**, 1064 (1977).
[27]J. C. Alonso, R. Vazquez, A. Ortiz, V. Pankov, and E. Andrade, J. Vac. Sci. Technol. A **16**, 2231 (1998).
[28]R. Henda, J. Vac. Sci. Technol. A **20**, 1369 (2002).
[29]K. Yamamoto, M. Tsuji, K. Washio, H. Kasahara, and K. Abe, J. Phys. Soc. Jpn. **52**, 925 (1983).
[30]C. J. Fang, L. Ley, H. R. Shanks, K. J. Gruntz, and M. Cardona, Phys. Rev. B **22**, 6140 (1980).
[31]P. N. Schatz and D. F. Horning, J. Chem. Phys. **21**, 1516 (1953).
[32]J. D. Jackson, *Classical Electrodynamics*, 2nd ed. (Wiley, New York, 1975), p. 152.
[33]G. A. N. Connel and J. R. Pawlik, Phys. Rev. B **13**, 787 (1976).